Advanced Optical Technologies

TYPE Original Research
PUBLISHED 29 December 2025
DOI 10.3389/aot.2025.1707828

OPEN ACCESS

EDITED BY
Philippe Velha,
University of Trento, Italy

REVIEWED BY
Dalton Müller Pessôa Filho,
São Paulo State University, Brazil
Pu-Chun Mo,
National Cheng Kung University, Taiwan
Hao-Nan Wang,
Sichuan University, China

*CORRESPONDENCE
Vanja Dvekar,
vdvekar@torontomu.ca

RECEIVED 18 September 2025
REVISED 07 December 2025
ACCEPTED 12 December 2025
PUBLISHED 29 December 2025

CITATION
Dvekar V, Sadrzadeh-Afsharazar F, DeVos L, Saiko G and Douplik A (2025) Near infrared spectroscopy assessment of wrist-based vascular occlusion protocols.
Adv. Opt. Technol. 14:1707828.
doi: 10.3389/aot.2025.1707828

Near infrared spectroscopy assessment of wrist-based vascular occlusion protocols

Vanja Dvekar[1]*, Faraz Sadrzadeh-Afsharazar[2], Leah DeVos[2], Gennadi Saiko[1] and Alexandre Douplik[1,3]

[1]Department of Physics, Toronto Metropolitan University (TMU), Toronto, ON, Canada, [2]Department of Biomedical Engineering, Toronto Metropolitan University (TMU), Toronto, ON, Canada, [3]Institue of Biomedical Engineering, Science and Technology (iBEST), Keenan Research Centre of the LKS Knowledge Institute, St. Michael's Hospital, Toronto, ON, Canada

Background: Vascular occlusion tests (VOTs) are widely used to assess microvascular function with near-infrared spectroscopy (NIRS), but protocols vary substantially, particularly in occlusion pressure and anatomical site. Most studies focus on the upper arm or thigh, with few studying distal limbs such as the wrist, highlighting the importance of standardizing wrist-based arterial occlusion pressures.
Methods: To address this gap, the present study examined the effects of two fixed occlusion pressures, 150 mmHg and 200 mmHg, applied at the wrist on the local muscle oxygenation dynamics. A total of 21 healthy participants underwent an 8-min experimental protocol comprising a 1-min baseline (no pressure), 3-min occlusion, and 4-min reperfusion period. Muscle oxygenation was continuously monitored from the thenar eminence of the occluded hand using a commercial near-infrared spectroscopy (NIRS) device (Moxy, Hutchinson, USA).
Results: Reactive hyperemia responses at the two pressures were compared for five distinct metrics: amplitude of muscle oxygen saturation (SmO_2) ($p = 0.0065$), time to maximum SmO_2 ($p = 0.235$), and three first-derivative features: time to peak slope ($p = 0.694$), peak slope value ($p = 0.019$), and full width at half maximum (FWHM) ($p = 0.46$). Statistically significant differences were observed in amplitude of SmO_2, and peak slope value. However, the temporal metrics such as time to max SmO_2, time at peak slope value, and FWHM, were not significantly different.
Conclusion: Overall, this study supports the potential of wrist-based AOP protocols and highlights the importance of selecting appropriate occlusion pressures and anatomical sites to optimize vascular response while minimizing patient discomfort. Given the wrist's anatomical advantages, incorporating wrist-based occlusion into daily practice and clinical assessments may enhance its translational potential as a pressure occlusion site.

KEYWORDS

arterial occlusion pressure, hemodynamic sensing, near infrared spectroscopy, reactive hyperemia, vascular occlusion

1 Introduction

Vascular occlusion tests (VOTs) are procedures in which blood flow to a limb or tissue is temporarily interrupted, using an inflatable cuff, to assess local tissue oxygenation and vascular reactivity (Niezen et al., 2022; Bezemer et al., 2009; Niezen et al., 2023). Traditionally, VOTs have been used in research involving imaging and optical technologies, such as ultrasound imaging and near-infrared spectroscopy (NIRS).(Niezen et al., 2022; Bezemer et al., 2009; Niezen et al., 2023; Harris et al., 2010; Willingham et al., 2016). NIRS has become a very popular tool in VOT, where common protocols include placing the device to the distal limbs, such as the forearm, hand, calf, or foot, with recommendation of the hand (thenar eminence) due to low levels of subcutaneous adipose tissue, glabrous skin, and good reproducibility amongst healthy participants (Mayeur et al., 2011; Gómez et al., 2009; Hendrick et al., 2024; Bezemer et al., 2009). Hemodynamic parameters frequently extracted from NIRS signals for analysis are oxygenated hemoglobin (HbO_2), total hemoglobin (tHb), tissue/muscle saturation/oxygenation index (StO_2, SmO_2, TSI), and area under the curve (AUC). This technology is commonly used alongside flow mediated dilation FMD, as a validation tool to provide different but complementary results (Hendrick et al., 2024).

Despite the extensive use of VOTs in research, the consensus on standardized protocols for VOTs remains limited, especially with respect to selecting appropriate cuff pressures, determining anatomical cuff placement, and accounting for participant comfort.

Across studies, considerable variability exists in the arterial occlusion pressures (AOP) and applications of sites. Pressures used during VOT's typically range from partial to suprasystolic AOP (Jessee et al., 2016; Willingham et al., 2016; Vehrs et al., 2024). Clinically, torniquete cuff pressures of upper and lower extremities are set to 10 mmHg above systolic blood pressure (SPB) for partial occlusion, or 250 mmHg–300 mmHg for complete occlusion (Sharma et al., 2014; Souza et al., 2025). Suprasystolic pressures, often used in research, may be unnecessarily large, leading to discomfort in participants, while partial pressures, although may associate with higher comfort, may not exhibit the same hemodynamic response (Sun et al., 2024). Recent NIRS studies have demonstrated that occlusion pressure influences hyperemic responses, with larger occlusion generating greater reperfusion kinetics than significantly low pressures applied (Desanlis et al., 2024). However, when comparing partial and suprasystolic pressures of arterial occlusion, the response of deoxygenation and re-oxygenation are not significantly impacted, suggesting lower pressures can be a more favourable approach to VOT's.

The upper arm and thigh have become favourable sites when performing VOTs as they induce large volume ischemia across the extended limb, however, this simultaneously increases the volume of pain sensitivity (Krishnan et al., 2011; Soares et al., 2018). This introduces an interesting topic of measuring distal limbs such as the wrist, however, minimal studies evaluate VOT testing in the wrist (Futier et al., 2011).

Physiologically, the wrist presents several advantages as an occlusion site compared with the upper arm. The wrist contains two long bones, the radius and ulna, which distribute cuff pressure more evenly than the single humerus at the upper arm, reducing localized compression of neurovascular structures and discomfort during suprasystolic inflation (Forro et al., 2023). Furthermore, the radius and ulnar arteries supply blood to the wrist and hands, which are intertwined within the two bones, this may reduce pressure to vasculature that run between the bones, and therefore reduce discomfort during occlusion. Wrist occlusion primarily interrupts blood flow to the hand and intrinsic musculature, whereas brachial occlusion halts perfusion to a larger tissue volume, increasing ischemic distress (Imms et al., 1988; Forro et al., 2023).

Furthermore, the wrist has become a common site in devices that measure various cardiovascular health parameters, as it is more accessible for repeated measurements. The wrist also offers improved feasibility in individuals with obesity or large arm circumferences, where upper-arm cuff placement may be less accurate or uncomfortable as well require larger occlusion pressures (Hyttel-Sorensen et al., 2014; Lende et al., 2021; Thomas et al., 2015; Cunniffe et al., 2017). These anatomical and vascular distinctions provide a physiological rationale for evaluating wrist-based AOP, particularly when participant comfort and protocol reproducibility are priorities.

Therefore, this study aims to evaluate NIRS-derived vascular responses to wrist-applied occlusion pressures of 150 mmHg and 200 mmHg. We hypothesize that 150 mmHg arterial occlusion pressure (AOP) will generate similar hemodynamic responses to a higher AOP of 200 mmHg while providing superior comfort, thereby supporting the wrist as a viable site for standardized VOT measurement.

2 Methods

2.1 Participants

This study was approved by the research ethics board, and written consent forms were obtained before each experiment. Twenty-one healthy participants (12 males and 9 females) were included in this study; Participants' ages were 25 ± 3 years, with a mean resting blood pressure of 119 ± 13/78 ± 14 mmHg for males and 105 ± 13/73 ± 7 mmHg for females. The exclusion criteria for this experiment were: injuries or musculoskeletal pain, cardiovascular health issues, and participation in exercise prior to the experiment.

2.2 Instrumentation

2.2.1 NIRS device

MOXY was used to detect SmO_2 during the experiment. The monitor consists of two detectors and a multi-wavelength emitter (see Figure 1 for wavelengths used), measuring SmO_2 at a sampling frequency of 1 Hz with a built-in 10 s smoothing average filter, in the probed muscle tissue. MOXY accounts for both myoglobin (Mb) and hemoglobin (Hb) when deriving muscle oxygenation through the following equation (Feldmann et al., 2019).

$$SmO_2 = \frac{MbO_2 + HbO_2}{tMb + tHb} \quad (1)$$

Where MbO_2 and HbO_2 represent oxymyoglobin and oxyhemoglobin, respectively. Total myoglobin (tMb) and total

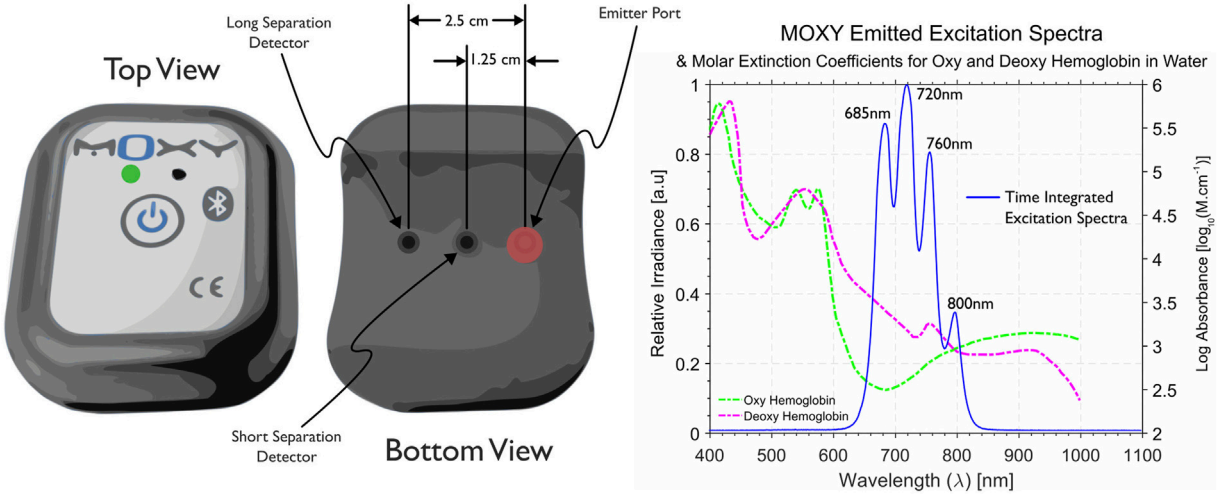

FIGURE 1
MOXY device and its optical properties. (Left) Top and bottom views of the MOXY device showing the emitter port, short-separation detector, and long-separation detector with corresponding source–detector distances (1.25 cm and 2.5 cm). (Right) Emitted excitation spectra of the MOXY device (blue line) overlaid with the molar extinction coefficients of oxyhemoglobin (green dashed line) and deoxyhemoglobin (magenta dashed line) in water, highlighting key wavelengths used for muscle oxygenation measurement.

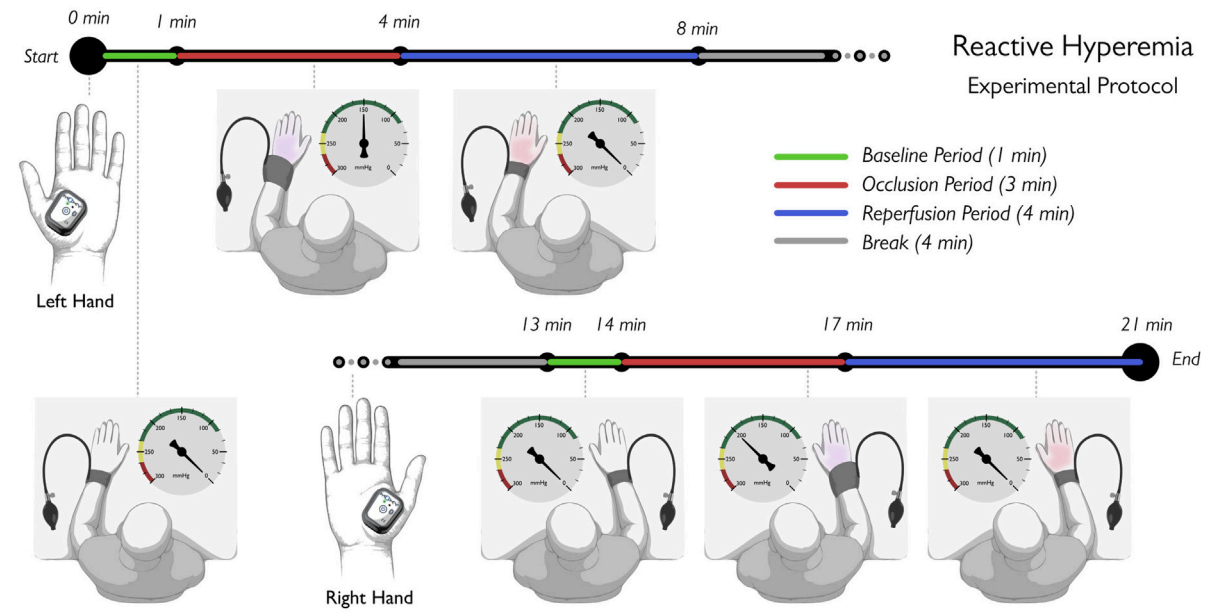

FIGURE 2
Experimental protocol with visual of MOXY placement and occlusion protocol.

hemoglobin (*tHb*) denote the sum of their oxygenated and deoxygenated forms. NIRS technology is unable to distinguish between *Mb* and *Hb*, nevertheless, because the absorption spectra of these chromophores are highly similar, SmO_2 can still be accurately derived from Equation 1 (Feldmann et al., 2019).

In the experimental design, MOXY was placed on the thenar eminence, a region characterized by a relatively high concentration of *Mb* due to its predominance of slow-twitch muscle fibers. Slow-twitch fibers are well documented to contain higher *Mb* concentrations compared to fast-twitch fibers, where in slow-twitch muscles the concentration of *Mb* is approximately 0.7 mM± 0.09 while in fast-twitch fibers it is reported to be 0.49 mM± 0.07 (Plotkin et al., 2021; Jansson and Sylvén, 1983; Bekedam et al., 2009). Consequently, the SmO_2 measurements obtained in this region of interest reflect greater myoglobin derived oxygen availability than would be expected in predominantly fast-twitch muscles.

2.3 Study design

2.3.1 Experimental design

Participants sit with their hands placed side by side on a raised platform in a prone position. A pressure cuff is placed around the wrist and the MOXY device is placed on the thenar eminence of the palm of the experimental hand (see Figure 2). The forearms were supported on a stable surface, and the hands were positioned on a raised support to maintain consistent probe to skin contact. This configuration provided gentle upward pressure on the NIRS device and minimized wrist and hand movement to reduce motion artifacts. Additionally, the thenar eminence is an important target for vascular reflex adaptation, having an earlier and more amplified vascular response than many other tissues, and little signal influence of skin and fat tissue. Additionally, as we target occlusion at the wrist, not many muscles with these advantages are present in these distal regions (Bezemer et al., 2009; Niezen et al., 2022; Payen et al., 2009).

2.3.2 Occlusion protocol

Each participant underwent two trials of data collection which is broken down in Figure 2. In the first trial, the left wrist was occluded at 150 mmHg for 3 min. After a 5-min rest, the procedure was repeated on the right hand at the occlusion pressure of 200 mmHg.

Our study intentionally selected two pressures that reflect distinct but meaningful points on the spectrum of 10 mmHg–300 mmHg AOP's. The wrist has a smaller circumeference and therefore these pressures may be sufficient enough based on previous studies and the relationship between limb circumference and pressure (Sharma et al., 2014; Cunniffe et al., 2017).

The lower pressure, 150 mmHg, corresponds to approximately 10–30 mmHg above resting systolic pressure. Prior studies have shown that 30 mmHg above systolic pressure is often sufficient to achieve arterial cessation in the upper limb, which aligns with our participants' mean systolic values (Sharma et al., 2014; Cunniffe et al., 2017) (see Supplementary Table S6).

The higher pressure, 200 mmHg, represents the lower boundary of the traditional body size independent suprasystolic pressures commonly used across studies Sharma et al. (2014); Cunniffe et al. (2017). This makes it a relevant comparator, as it is widely applied while still avoiding the excessively high pressures ($>250\,mmHg$) that may induce unnecessary discomfort or risk.

5-min rest periods between the experiments for each hand were chosen based on previous literature (Thomson et al., 2009; Smielewski et al., 1997; Lubiak et al., 2025) where Sharma et al. (2014) showed that 5 min was a sufficient time to return to baseline.

Two arms were used in this experiment to avoid repeated pressure on a single arm. Due to the small sample size, the testing sequence was fixed, left hand followed by right, to ensure procedural consistency and reduce inter-participant variability.

2.3.3 Data collection

Data collection followed the same steps for each occlusion condition: Baseline: A 1-min baseline reading was collected with no cuff pressure. During the Occlusion Period: The wrist cuff was inflated to the target pressure (150 mmHg left hand or 200 mmHg right hand) and held for 3 min. Finally, during the Reperfusion Period: The cuff was deflated, and SmO_2 was monitored for 4 min. At the 8-min mark, data collection was stopped. After a 5-min rest, the protocol was repeated on the contralateral limb seen in Figure 2.

2.4 Signal overview

An example signal from the MOXY is depicted in Figure 3. The baseline reading is taken for 1 min, where there are no changes in blood oxygen saturation. Following baseline, occlusion occurs for a 3-min period, where the arterial flow is diminished, causing a decrease in oxygenated blood. During post-occlusion, there is a significant reperfusion to previously occluded areas; this is due to reactive hyperemia, leading to a transient increase in arterial diameter, causing an overshoot in oxygenation.

2.5 Signal processing

Signal processing methods were applied using MATLAB 2023b Software (Mathworks, Natick, MA, USA) to the MOXY data following acquisition to improve signal quality. The raw data was smoothed using a filter implemented via MATLAB's `smooth` function, with a window size of 5, to reduce high-frequency noise. Outliers were then identified and corrected using the `filloutliers` function, which replaces aberrant points with values obtained through linear interpolation between neighbouring non-outlier samples. This approach removes significant signal fluctuations while preserving the physiological and temporal characteristics of the hemodynamic response.

To standardize the data across participants and facilitate comparison, all reactive hyperemic signals were isolated and baseline-corrected by setting the initial x (time) and y (signal) values to zero. This was implemented in MATLAB by subtracting the first value of the time vector from all subsequent time points and subtracting the first signal value from all subsequent signal measurements. This procedure ensured that all signals started from a common origin, preserving the shape and dynamics of the hemodynamic response while removing offsets. The first derivative test was performed on the reactive hyperemic component using the MATLAB 2023b Software (Mathworks, Natick, MA, USA). The numerical gradient function was used as it estimates the partial derivatives in each dimension using the function's known values at specific points. To compute the first derivative, the function grad(x) was used in MATLAB where $\partial F/\partial x$ finds the differences in the x (horizontal) direction of the muscle oxygen saturation.

2.6 Data analysis

The primary analysis is performed on the RH period seen in Figure 3a. The time zero-point was reset at the commencement of the reperfusion period. From the SmO_2 time series during the RH period, maximum muscle oxygenation (Max SmO_2), and time to maximum oxygenation were extracted while the first

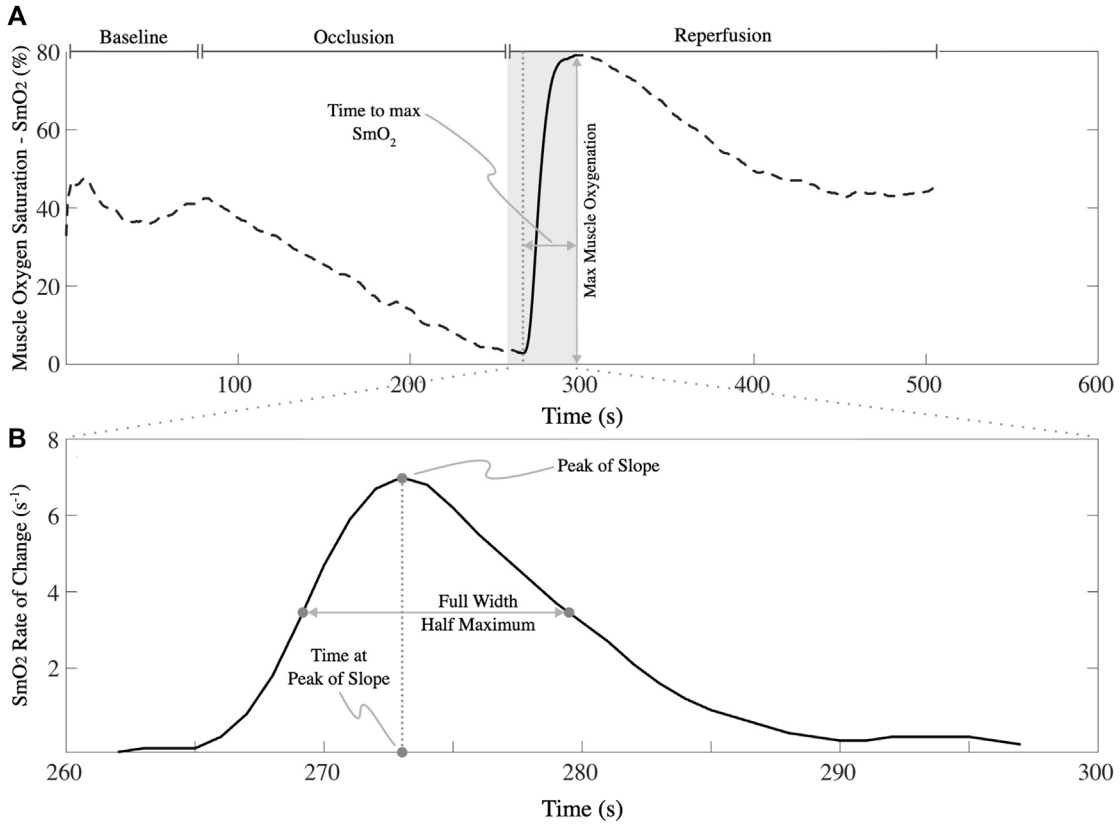

FIGURE 3
Sample data of muscle oxygenation (SmO_2) dynamics during the experiment. **(a)** top graph shows SmO_2 signal across: baseline, occlusion, and reperfusion. Key features include time to maximum SmO_2 and reactive hypermic (RH)-induced peak SmO_2. **(b)** bottom graph shows first time derivative of SmO_2 during reperfusion, highlighting the peak slope, time at peak slope, and full width at half maximum (FWHM), additional key metrics used for post-analysis.

derivative was used to obtain the peak slope (maximum $dSmO_2/dt$), its timing, and the full width at half maximum (FWHM), which can be visualized in Figure 3b.

The amplitude reflects the overall change in oxygen saturation, while time to maximum indicates the delay to peak oxygenation. Peak slope and time to peak slope quantify the rate and timing of oxygen delivery, and FWHM measures the duration of elevated SmO_2. Together, these parameters capture both the magnitude and temporal characteristics of microvascular function following cuff release.

These parameters are commonly assessed in VOT's, particularly the upslope, time to maximum saturation, and area under the curve (AUC). To enable more detailed analysis, additional measurements of the AUC were calculated for the ascending phase, peak, and descending phase of the SmO_2 response, capturing both the magnitude and duration of oxygenation changes throughout reperfusion.

2.7 Statistical analysis

The following information on statistical analysis tree is illustrated in Figure 4 and findings for normality leading to statistical test used are also shown in Table 1.

2.7.1 Target sample size calculation

The sample size was calculated using a power of 0.80 and an alpha value of 0.05. For each metric, the 21 samples were used to determine the effect size, followed by the sample size, by using the means and pooled standard deviation of 150 mmHg and 200 mmHg for each metric. This test was done on the preliminary data collected, as current data on muscle oxygenation for the wrist occlusion is not available.

2.7.2 Statistical test decision tree

DATAtab (DATAtab, Austria) was used to statistically compare the 150 and 200 mmHg scenarios. The Shapiro-Wilk method was used to test for normality as the primary modality. If the results presented contradictory results, a non-normality test was performed.

Following the normality test, if the distributions were deemed not normal for both or one hand, a Wilcoxon paired test would be performed, while if there were a normal distribution for both hands, then a paired t-test would be conducted.

2.7.3 Wilcoxon paired test and paired T-test

A Wilcoxon paired test and two-tailed paired t-tests were computed for the sample size to analyze the statistical difference between the pressures on the wrist. The null hypothesis inferred that

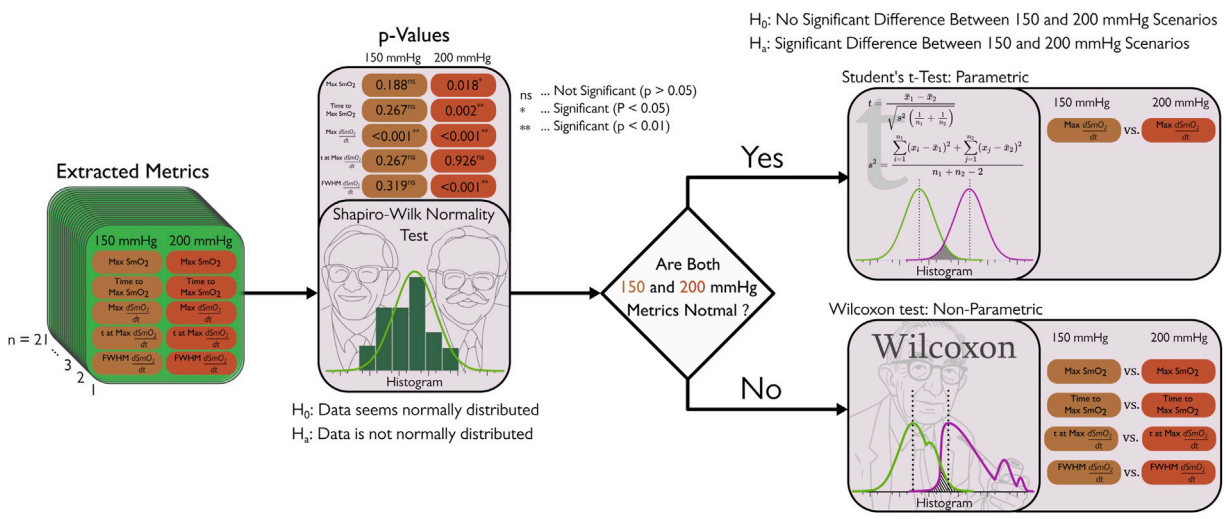

FIGURE 4
Statistical decision tree used to determine the appropriate comparative test for each extracted metric of number (n) participants. Normality of data from both occlusion pressures (150 and 200 mmHg) was assessed using the Shapiro–Wilk test. If both datasets met the assumption of normality by non-significance (ns), a parametric Student's t-test was applied to evaluate differences between conditions. If either dataset violated normality, a non-parametric Wilcoxon signed-rank test was used instead. This flowchart summarizes the analytical pathway followed to ensure appropriate statistical test selection for all NIRS-derived metrics.

TABLE 1 Normality for each metric determined followed by the statistical test used.

Metric	Normality	Test used
Max muscle oxygenation	No	Wilcoxon paired
Time to maximum oxygenation	No	Wilcoxon paired
Time at peak slope value	No	Wilcoxon paired
Peak of slope value	Yes	T-test paired
Full width half maximum	No	Wilcoxon paired

the mean for all participants did not differ between 150 mmHg and 200 mmHg pressures. The alternative hypothesis states that there is a difference between these pressures. The statistical significance can be determined where α, or the significance level, was set at 0.05. If the p-value $< \alpha$, the null hypothesis is rejected, and if the p-value $\geq \alpha$, we fail to reject the null hypothesis. For this study, statistical analysis is performed on DataTab to find the significance of applying different pressures on the wrist.

3 Results

The normality of data was determined to decide the nature of the statistical test to be used (see Supplementary Materials). As there was a mix of normality amongst the metrics analyzed, both parametric testing (t-test) and non-parametric test (Wilcoxon paired) were used. The metrics investigated were acquired from each participant's data for the RH component (see Figure 5 for visualization depth of data collected). The RH component provides information on the oxygen saturation within muscle tissue, whilst the first derivative test provides deeper vasculature information.

Figures 6, 7 illustrate how each metric changes with the pressure. The Max SmO_2 and peak of slope value from the derivative of the RH component when comparing 150–200 mmHg suggest statistical significance, while the remaining metrics, time to max muscle oxygen saturation, time at peak slope, and FWHM do not display statistically significant results. (See Table 2 for summary of all results).

Statistically significant differences were observed in the maximum SmO_2 and peak of slope value (max SmO_2 rate of change) across participants, indicating that higher occlusion pressures enhance both the magnitude and the rate of oxygen resaturation during reperfusion. Physiologically, a more substantial ischemic stimulus is produced from the larger pressure cuff, as there is greater vasodilation and a more robust reactive hyperemic response upon cuff release. This means that the larger pressure not only increased the oxygenation but it also increased the number of vasodilators to ensure a larger rush of blood.

In contrast, there are no significant differences in the temporal metrics analyzed (time to maximum SmO_2, time to peak slope, and FWHM). This indicated that although the magnitude of the RH response increased at higher occlusion pressures, the timing remained conserved. Although the amount of HbO_2 available to sustain the occluded limb varies with pressure, this does not alter the time required for oxygenated blood to reach the muscle upon cuff release. This suggests that the magnitude of oxygen delivery, rather than its temporal dynamics, more strongly influences the hemodynamic response at these pressures.

4 Discussion

The main findings of our study are that our maximum SmO_2 and the maximum rate of change of SmO_2 (peak slope) show statistically significant responses to the different pressures

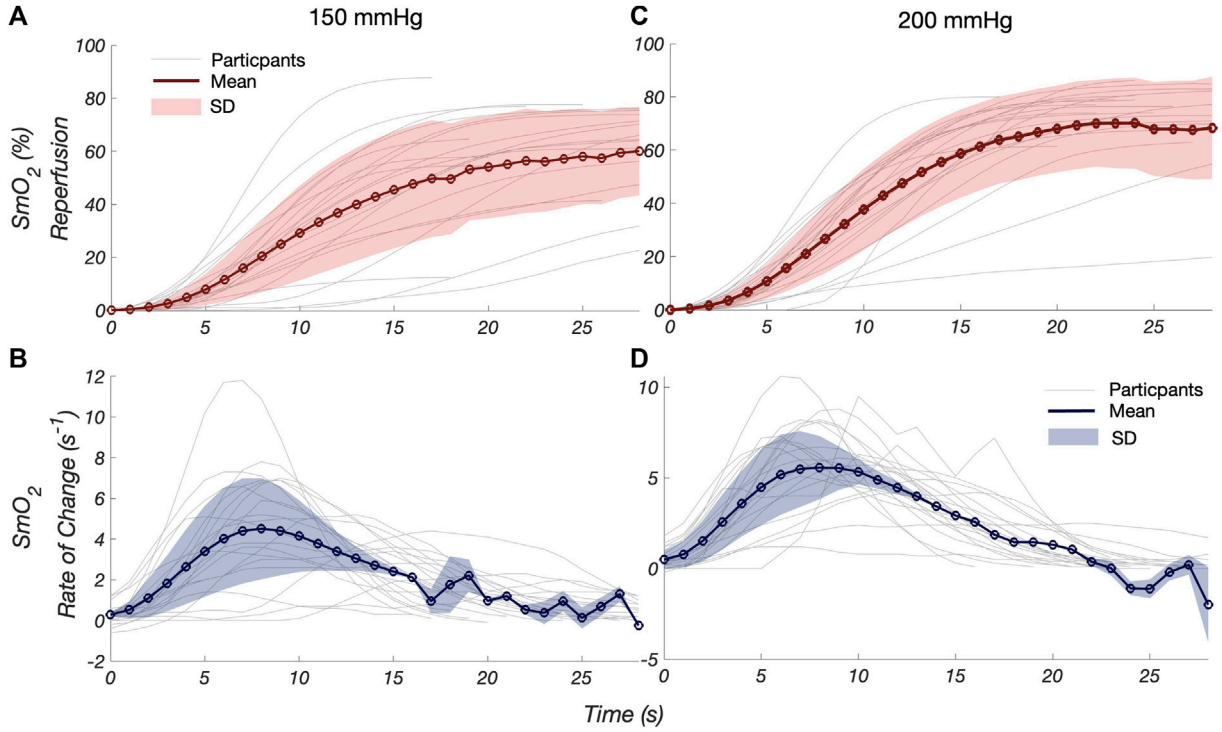

FIGURE 5
Muscle oxygenation (SmO_2) and rate of change of SmO_2 data collected for 21 participants (grey line) with Mean (solid line with circle marks) ± standard deviation (SD) (band around solid line): **(a)** SmO_2 for 150 mmHg, **(b)** rate of change of SmO_2 for 150 mmHg, **(c)** SmO_2 for 200 mmHg, **(d)** rate of change of SmO_2 for 200 mmHg.

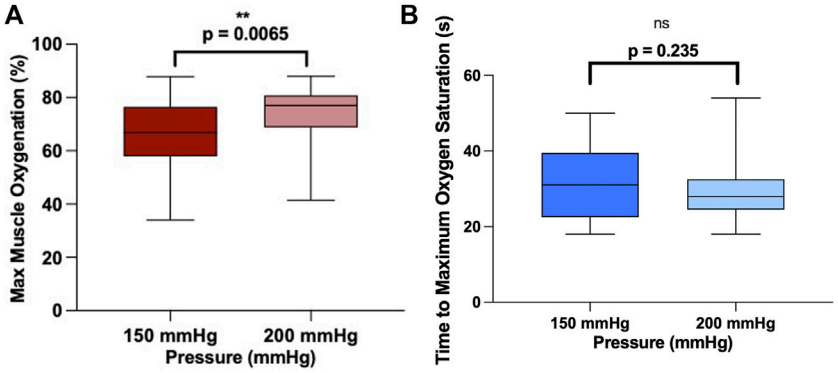

FIGURE 6
Boxplots of metrics from the reactive hyperemic (RH) component: **(a)** Maximum muscle oxygenation in percent (%) (150 mmHg: 61.2 ± 18.4, 200 mmHg: 73.6 ± 10.4; $p = 0.0065$) and **(b)** Time to maximum muscle oxygenation in seconds (s) (150 mmHg: 31.0 ± 9.47, 200 mmHg: 28.4 ± 8.53; $p = 0.235$). Data are presented as occlusion pressure: mean ± SD; p-value across participants ($n = 21$). Figure generated using GraphPad Prism (GraphPad Software, San Diego, CA, USA).

applied, with $p = 0.0065$ and $p = 0.019$, respectively. The mean for the two metrics at an AOP of 200 mmHg was larger than 150 mmHg (maximum SmO_2: 74.1 ± 10.5 vs. 65.3 ± 13.41; maximum $dSmO_2/dt$: 6.5 ± 2.08 vs. 5.10 ± 2.44), suggesting that the amount of oxygen present at the thenar eminence at the time after ischemia increases with larger pressures. The influence of pressure on the time to the maximum SmO_2 ($p = 0.235$), the time at the peak slope ($p = 0.694$), and FWHM ($p = 0.46$) did not differ significantly, indicating that the time for the blood to reach the thenar eminence, although varied between means, did not have statistical significance between the two groups.

These results imply that at 150 mmHg and 200 mmHg, the magnitude of reperfusion response is amplified without substantially altering the timing of vascular recovery. This may occur because the $SmO2$ recovery slope reflects the microvascular blood flow response to induced ischemia, leading to an increased oxygen deficit at higher

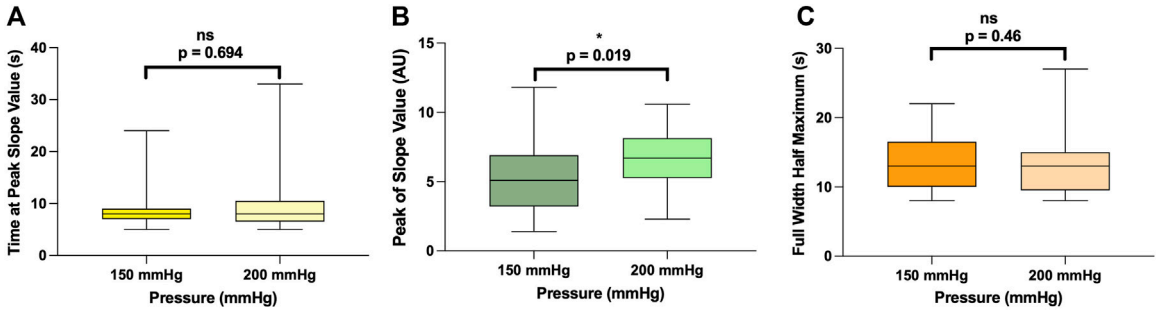

FIGURE 7
Boxplots of metrics from the first derivative of the reactive hyperemic (RH)component: **(a)** Time at peak of slope value in seconds (s) (150 mmHg: 9.57 ± 5.21, 200mmHg: 10.3 ± 6.45; $p = 0.235$), **(b)** Peak of slope value in arbitrary units (AU) (150 mmHg: 5.11 ± 2.44, 200mmHg: 6.51 ± 2.080; $p = 0.019$), and **(c)** Full width half maximum in seconds (s) (150 mmHg: 14.1 ± 3.73, 200mmHg: 13.5 ± 4.05; $p = 0.019$). Data are presented as occlusion pressure: mean ± SD; p-value across participants ($n = 21$). Generated using GraphPad Software, San Diego, CA, USA.

TABLE 2 Summary of results found for each metric, including mean ± SD for each pressure, the statistical test performed, and the corresponding p-value.

Metric	Mean ± SD 150 mmHg	Mean ± SD 200 mmHg	Test type	P-value
Max muscle oxygenation	61.2 ±18.4	73.6 ±10.4	Wilcoxon paired	0.0065
Time to max muscle oxygenation	31.0 ±9.47	28.4 ±8.53	Wilcoxon paired	0.235
Time at peak slope value	9.57 ±5.21	10.3 ±6.45	Wilcoxon paired	0.694
Peak of slope value	5.11 ±2.44	6.51 ±2.08	T-test paired	0.019
Full width half maximum	14.1 ±3.73	13.5 ±4.05	Wilcoxon paired	0.46

pressures. Furthermore, as constriction increases, accumulation of vasodilators such as H+ ions, prostaglandins, K+ ions, bradykinin, endothelium-derived hyperpolarization factor and nitric oxide increase, promoting a greater oxygen supply. (Coccarelli and Nelson, 2023; Dakak et al., 1998) Endothelial NO is critical for vasodilation; inhibition of NO reduces the peak reactive hyperemic response. At higher occlusion pressures, shear stress may be more pronounced, further increasing NO-mediated dilation and thus increasing the volume of oxygenated hemoglobin passing through (Coccarelli and Nelson, 2023; Dakak et al., 1998).

During reactive hyperemia, microvascular recruitment and capillary refill govern the rapid rise in oxygenation measured by NIRS post cuff release. When arterial inflow is occluded, vasodilators accumulate and propagate upstream from capillaries to terminal arterioles (Horn et al., 2022; Coccarelli and Nelson, 2023). Once the cuff is released, these arterioles dilate, allowing a surge of red blood cells to refill perfused capillaries. This post-occlusion refill is the source of the steep re-oxygenation detected by NIRS. Capillary recruitment is heterogeneous, with some arteriole branches reopening fully while others remain constricted, producing regions of no flow. This heterogeneity can modulate the magnitude and rate of reoxygenation (Horn et al., 2022). In this study, a steep re-oxygenation was observed across the different pressures applied, which did not significantly affect the time metrics.

Desanlis et al. (2024), used NIRS to compare pressures in the upper arm (G1: 50 mmHg, G2: systolic blood pressure + 50 mmHg, G3: 250 mmHg). They performed 3 cycles of 7 min occlusions. After cuff deflation, the tissue saturation index (TSI max), was statistically different between G1 and G2, G1 and G3, but not between G2 and G3. However, the max TSI values showed that the overall PORH mean was higher as pressure increased from G1 to G3 such as in session 1 ($G1$: 1.933 ± 2.01 < $G2$: 9.54 ± 3.274 < $G3$: 12.219 ± 1.485). The TSI AUC (arbitrary units A.U.) and TSI time (seconds s) showed no significant differences between G2 and G3, ($G2$ = 961.425 ± 296.556 *a.u.*; $G3$ = 1007.45 ± 228.827 *a.u.*), ($G2$ = 15.267 ± 6.064*s*; $G3$ = 14.779 ± 4.899 *s*); As they investigated the speed of reperfusion, they found that there was a significant difference between G2 and G3 where G3 had a steeper slope ($G3$: 1.264 ± 0.147 *vs.* $G21.044$ ± 0.209).

Similar results were seen in our study; statistical significance was determined for maximum SmO2, unlike in (Desanlis et al., 2024), however, the same trend was observed where with the larger pressure there was a larger SmO_2 percentage. The time to max SmO_2 showed no statistical significance between the pressures, however at a higher pressure, the mean time was shorter (150 $mmHg$: 32.0 ± 9.47 > 200 $mmHg$: 29.42 ± 8.53). The peak of slope value (%/*s*) was significantly different between the pressures, which (Desanlis et al., 2024) also observed, and the mean values were also larger at higher pressures, similar to this previous study.

Another study observed the minimum cuff pressure required to cause observable changes in brachial and popliteal flow in 42 healthy males (Souza et al., 2025). Cuff pressures were increased in increments from rest (0–100 mmHg) at intervals of 20 mmHg and then by 10 mmHg until blood flow was occluded. This study used 2D B-mode ultrasound imaging to detect blood flow changes.

Significant reductions in blood flow were observed at 120 mmHg for the brachial artery and at 110 mmHg for the popliteal artery. This suggested that reduction of blood flow occurred above 110 and 120, for each anatomical site, respectively. This supports the dependence of pressure on hemodynamic response, as seen in our max SmO_2 and max rate of change of SmO_2, with two of the five metrics influenced by pressure (Didier et al., 2020; Souza et al., 2025).

Although pressure dependence is similar, the primary issue stems from the validity of comparing metrics between anatomical sites. Many studies examine the upper arm and lower limbs with minimal attention to wrist sites, so physiologically, these differences can affect the final hemodynamic response. This was also suggested in studies related to blood flow flux, suggesting it was shorter in skeletal muscles than in the brachial arteries, and that the pressure required to halt arterial blood flow in the brachial artery was different from that in the popliteal artery (Didier et al., 2020; Souza et al., 2025). The need to further study the wrist as an occlusion site should be pursued, as it may be beneficial for future implementation into clinical and rehabilitative applications. Such applications can include non-invasive monitoring of microvascular health, tracking endothelial function in patients with cardiovascular or metabolic disease, guiding individualized occlusion pressures during blood-flow-restriction rehabilitation, and enabling standardized, low-burden vascular assessments in clinical and community settings. Furthermore, investigation of its comfort can significantly benefit the willingness of participants to perform VOTs more readily. These findings highlight the need for further investigation of the wrist as an occlusion site.

5 Limitations

Our study has several limitations. The sample size (n = 21; target = 40) limits statistical power and may reduce the ability to detect minor effects. Participant comfort was not quantitatively assessed, preventing evaluation of pressure-related tolerability. Inter-individual variability, including sex, blood pressure, and probe placement, was not controlled and may have influenced the SmO_2 responses. Occlusion was applied to a non-randomized hand, potentially introducing side-dominance bias. Probe pressure inconsistencies may also have affected the accuracy of NIRS measurements. This study was conducted under strictly static conditions with the wrist and hand immobilized to minimize motion artifacts. However, during dynamic movement, the wrist and forearm exhibit substantial biomechanical variability including changes in joint angle, muscle recruitment, and tissue compression that can alter the applied cuff pressure and influence hemodynamic responses. These factors make it difficult to standardize the occlusion protocol during motion. Therefore, the findings of this study should be interpreted as applicable only to non-moving protocols, and generalization to dynamic or exercise conditions remains highly limited.

Baseline SmO_2 normalization was not performed, potentially increasing inter-subject variability. Additionally, the fixed 5-min rest period did not confirm whether SmO_2 fully returned to baseline before subsequent trials, raising the possibility of cumulative vascular effects across repeated occlusions.

6 Future directions

Future studies should normalize baseline SmO_2, verify steady-state recovery before each occlusion, and use larger cohorts with randomized or crossover designs to improve reproducibility. Standardizing probe placement, reducing hand motion, and quantifying participant comfort will help reduce variability and improve protocol feasibility.

Expanding the analysis to include full reperfusion curve modeling and curve-fitting approaches will allow broader comparison between NIRS derived metrics and gold-standard assessments such as FMD. Incorporating established vascular function indices, such as FMD or time-to-half recovery, will help validate wrist-based NIRS measurements, strengthen physiological interpretation, and support standardized occlusion protocols specific to the wrist.

7 Conclusion

This study highlights the influence of occlusion pressure on vascular responses at the wrist. The wrist is a promising anatomical site because it is easily accessible and has a smaller circumference, which may allow for lower-pressure occlusions while maintaining an adequate ischemic stimulus. Expanding assessment at this site could support clinical and rehabilitative applications, including monitoring microvascular health and vascular function in populations at risk for cardiovascular disease, endothelial dysfunction, diabetes, or obesity. These findings suggest that further research is warranted to explore wrist-based VOT testing and the potential for standardized measurement of arterial occlusion pressure using NIRS, while considering the exploratory nature of the study and its limited sample size.

Data availability statement

The raw data supporting the conclusions of this article will be made available by the authors, without undue reservation.

Ethics statement

The studies involving humans were approved by Toronto Metropolitan University Research Ethics Board of Approval. The studies were conducted in accordance with the local legislation and institutional requirements. The participants provided their written informed consent to participate in this study.

Author contributions

VD: Writing – original draft, Writing – review and editing. FS-A: Writing – review and editing. LD: Writing – review and editing. GS: Writing – review and editing. AD: Writing – review and editing.

Funding

The author(s) declared that financial support was received for this work and/or its publication. The authors acknowledge funding from NSERC Alliance (AD), NSERC I2I (AD and GS), NSERC Personal Discovery grants (AD and GS), and Toronto Metropolitan University Faculty of Science Discovery Accelerator program grants (AD and GS) and Toronto Metropolitan University Health Research Fund (AD).

Acknowledgements

The authors thank all members of the Toronto Metropolitan University (TMU) Photonics lab for their valuable support and participation throughout this project. The authors also acknowledge the guidance and feedback provided by our supervisors, Alexandre Douplik and Gennadi Saiko, which greatly enhanced the quality of this work.

Conflict of interest

The author(s) declared that this work was conducted in the absence of any commercial or financial relationships that could be construed as a potential conflict of interest.

Generative AI statement

The author(s) declared that generative AI was not used in the creation of this manuscript.

Any alternative text (alt text) provided alongside figures in this article has been generated by Frontiers with the support of artificial intelligence and reasonable efforts have been made to ensure accuracy, including review by the authors wherever possible. If you identify any issues, please contact us.

Publisher's note

Supplementary material

The Supplementary Material for this article can be found online at: https://www.frontiersin.org/articles/10.3389/aot.2025.1707828/full#supplementary-material

References

Bekedam, M. A., van Beek-Harmsen, B. J., van Mechelen, W., Boonstra, A., and van der Laarse, W. J. (2009). Myoglobin concentration in skeletal muscle fibers of chronic heart failure patients. *J. Appl. Physiology* 107, 1138–1143. doi:10.1152/japplphysiol.00149.2009

Bezemer, R., Lima, A., Myers, D., Klijn, E., Heger, M., Goedhart, P. T., et al. (2009). Assessment of tissue oxygen saturation during a vascular occlusion test using near-infrared spectroscopy: the role of probe spacing and measurement site studied in healthy volunteers. *Crit. Care* 13, S4. doi:10.1186/cc8002

Coccarelli, A., and Nelson, M. D. (2023). Modeling reactive hyperemia to better understand and assess microvascular function: a review of techniques. *Ann. Biomedical Engineering* 51, 479–492. doi:10.1007/s10439-022-03134-5

Cunniffe, B., Sharma, V., Cardinale, M., and Yellon, D. (2017). Characterization of muscle oxygenation response to vascular occlusion: implications for remote ischaemic preconditioning and physical performance. *Clin. Physiology Functional Imaging* 37, 785–793. doi:10.1111/cpf.12353

Dakak, N., Husain, S., Mulcahy, D., Andrews, N. P., Panza, J. A., Waclawiw, M., et al. (1998). Contribution of nitric oxide to reactive hyperemia: impact of endothelial dysfunction. *Hypertension* 32, 9–15. doi:10.1161/01.hyp.32.1.9

Desanlis, J., Gordon, D., French, C., Calveyrac, C., Cottin, F., and Gernigon, M. (2024). Effects of occlusion pressure on hemodynamic responses recorded by near-infrared spectroscopy across two visits. *Front. Physiology* 15, 1441239. doi:10.3389/fphys.2024.1441239

Didier, K. D., Hammer, S. M., Alexander, A. M., Caldwell, J. T., Sutterfield, S. L., Smith, J. R., et al. (2020). Microvascular blood flow during vascular occlusion tests assessed by diffuse correlation spectroscopy. *Exp. Physiology* 105, 201–210. doi:10.1113/EP087866

Feldmann, A., Schmitz, R., and Erlacher, D. (2019). Near-infrared spectroscopy-derived muscle oxygen saturation on a 0% to 100% scale: reliability and validity of the moxy monitor. *J. Biomedical Optics* 24, 115001. doi:10.1117/1.JBO.24.11.115001

Forro, S. D., Munjal, A., and Lowe, J. B. (2023). "Anatomy, shoulder and upper limb, arm structure and function," in *StatPearls* (Treasure Island, FL: StatPearls Publishing).

Futier, E., Christophe, S., Robin, E., Petit, A., Pereira, B., Desbordes, J., et al. (2011). Use of near-infrared spectroscopy during a vascular occlusion test to assess the microcirculatory response during fluid challenge. *Crit. Care* 15, R214. doi:10.1186/cc10449

Gómez, H., Mesquida, J., Simon, P., Kim, H. K., Puyana, J. C., Ince, C., et al. (2009). Characterization of tissue oxygen saturation and the vascular occlusion test: influence of measurement sites, probe sizes and deflation thresholds. *Crit. Care* 13, S3. doi:10.1186/cc8001

Harris, R. A., Nishiyama, S. K., Wray, D. W., and Richardson, R. S. (2010). Ultrasound assessment of flow-mediated dilation. *Hypertension* 55, 1075–1085. doi:10.1161/HYPERTENSIONAHA.110.150821

Hendrick, E., Jamieson, A., Chiesa, S. T., Hughes, A. D., and Jones, S. (2024). A short review of application of near-infrared spectroscopy (nirs) for the assessment of microvascular post-occlusive reactive hyperaemia (porh) in skeletal muscle. *Front. Physiology* 15, 1480720. doi:10.3389/fphys.2024.1480720

Horn, A. G., Schulze, K. M., Weber, R. E., Barstow, T. J., Musch, T. I., Poole, D. C., et al. (2022). Post-occlusive reactive hyperemia and skeletal muscle capillary hemodynamics. *Microvasc. Research* 140, 104283. doi:10.1016/j.mvr.2021.104283

Hyttel-Sorensen, S., Hessel, T. W., and Greisen, G. (2014). Peripheral tissue oximetry: comparing three commercial near-infrared spectroscopy oximeters on the forearm. *J. Clinical Monitoring Computing* 28, 149–155. doi:10.1007/s10877-013-9507-9

Imms, F., Lee, W.-S., and Ludlow, P. (1988). Reactive hyperaemia in the human forearm. *Q. J. Exp. Physiology Transl. Integration* 73, 203–215. doi:10.1113/expphysiol.1988.sp003133

Jansson, E., and Sylvén, C. (1983). Myoglobin concentration in single type i and type ii muscle fibres in man. *Histochemistry* 78, 121–124. doi:10.1007/BF00491118

Jessee, M. B., Buckner, S. L., Dankel, S. J., Counts, B. R., Abe, T., and Loenneke, J. P. (2016). The influence of cuff width, sex, and race on arterial occlusion: implications for blood flow restriction research. *Sports Med.* 46, 913–921. doi:10.1007/s40279-016-0473-5

Krishnan, A., Lucassen, E. B., Hogeman, C., Blaha, C., and Leuenberger, U. A. (2011). Effects of limb posture on reactive hyperemia. *Eur. Journal Applied Physiology* 111, 1415–1420. doi:10.1007/s00421-010-1769-z

Lende, M. N., Feustel, P. J., Alafifi, R. L., and Lynch, T. A. (2021). Impact of obesity on blood pressures measured at alternative locations during pregnancy. *Am. J. Obstetrics and Gynecol. MFM* 3, 100441. doi:10.1016/j.ajogmf.2021.100441

Lubiak, S. M., Howard, M. A., Schmidt, J. T., Patel, N. N., Prajapati, A. J., Shah, N. M., et al. (2025). Time-course and pressure-dependent changes in microvascular responses during ischemic preconditioning. *Microvasc. Res.* 161, 104831. doi:10.1016/j.mvr.2025.104831

Mayeur, C., Campard, S., Richard, C., and Teboul, J.-L. (2011). Comparison of four different vascular occlusion tests for assessing reactive hyperemia using near-infrared spectroscopy. *Crit. Care Med.* 39, 695–701. doi:10.1097/CCM.0b013e318206d256

Niezen, C., Massari, D., Vos, J., and Scheeren, T. (2022). The use of a vascular occlusion test combined with near-infrared spectroscopy in perioperative care: a systematic review. *J. Clin. Monit. Comput.* 36, 933–946. doi:10.1007/s10877-021-00779-w

Niezen, C. K., Vos, J. J., Bos, A. F., and Scheeren, T. W. (2023). Microvascular effects of oxygen and carbon dioxide measured by vascular occlusion test in healthy volunteers. *Microvasc. Research* 145, 104437. doi:10.1016/j.mvr.2022.104437

Payen, D., Luengo, C., Heyer, L., Resche-Rigon, M., Kerever, S., Damoisel, C., et al. (2009). Is thenar tissue hemoglobin oxygen saturation in septic shock related to macrohemodynamic variables and outcome? *Crit. Care* 13, S6. doi:10.1186/cc8004

Plotkin, D. L., Roberts, M. D., Haun, C. T., and Schoenfeld, B. J. (2021). Muscle fiber type transitions with exercise training: shifting perspectives. *Sports* 9, 127. doi:10.3390/sports9090127

Sharma, V., Cunniffe, B., Verma, A. P., Cardinale, M., and Yellon, D. (2014). Characterization of acute ischemia-related physiological responses associated with remote ischemic preconditioning: a randomized controlled, crossover human study. *Physiol. Reports* 2, e12200. doi:10.14814/phy2.12200

Smielewski, P., Czosnyka, M., Pickard, J. D., and Kirkpatrick, P. (1997). Clinical evaluation of near-infrared spectroscopy for testing cerebrovascular reactivity in patients with carotid artery disease. *Stroke* 28, 331–338. doi:10.1161/01.str.28.2.331

Soares, R. N., George, M. A., Proctor, D. N., and Murias, J. M. (2018). Differences in vascular function between trained and untrained limbs assessed by near-infrared spectroscopy. *Eur. Journal Applied Physiology* 118, 2241–2248. doi:10.1007/s00421-018-3955-3

Souza, H. L., Wilk, M., de Oliveira, G. T., Bichowska-Pawęska, M., Bernardes, B. P., Dos Prazeres, E. O., et al. (2025). Determining minimum cuff pressure required to reduce arterial blood flow at rest. *Sci. Rep.* 15, 14322. doi:10.1038/s41598-025-99334-9

Sun, Z.-j., Chen, C.-h., Tan, Z.-l., Li, C.-r., Fei, H., Yu, X., et al. (2024). Personalized tourniquet pressure *versus* uniform tourniquet pressure in orthopedic trauma surgery of extremities: a prospective randomized controlled study protocol. *Contemp. Clin. Trials Commun.* 42, 101376. doi:10.1016/j.conctc.2024.101376

Thomas, S. S., Nathan, V., Zong, C., Soundarapandian, K., Shi, X., and Jafari, R. (2015). Biowatch: a noninvasive wrist-based blood pressure monitor that incorporates training techniques for posture and subject variability. *IEEE Journal Biomedical Health Informatics* 20, 1291–1300. doi:10.1109/JBHI.2015.2458779

Thomson, S., Al-Subaie, N., Hamilton, M., Cowan, M., Musa, S., Grounds, R., et al. (2009). Adaptability of muscle tissue oxygenation to repeated vascular occlusion. *Crit. Care* 13, P241. doi:10.1186/cc7405

Vehrs, P. R., Hager, R., Richards, N. D., Richards, S., Baker, L., Burbank, T., et al. (2024). Measurement of arterial occlusion pressure using straight and curved blood flow restriction cuffs. *Physiol. Rep.* 12, e16119. doi:10.14814/phy2.16119

Willingham, T. B., Southern, W. M., and McCully, K. K. (2016). Measuring reactive hyperemia in the lower limb using near-infrared spectroscopy. *J. Biomedical Optics* 21, 091302. doi:10.1117/1.JBO.21.9.091302